Journal of American Science

Websites:
http://www.jofamericanscience.org
http://www.sciencepub.net

Emails:
editor@sciencepub.net
sciencepub@gmail.com

MARSLAND PRESS
Multidisciplinary Academic Journal Publisher

GENERATION OF NANO-/MICROSTRUCTURES OF CdS AND ZnO USING ELECTRODEPOSITION AND THEIR CHARACTERIZATION

*Sangeeta and **Dr. Vipin Kumar

*Research Scholar, Department of Physics, SunRise University, Alwar, Rajasthan (India)
** Professor, Department of Physics, SunRise University, Alwar, Rajasthan (India)
Email: rao.sangeeta1993@gmail.com

Abstract: The membranes used here as templates were of Makrofol KG foil (polycarbonate from Bayer AG), 10 µm thick, having an average pore diameter ~2 µm with pore density 2×10^6 cm^{-2}. This was prepared by irradiating the foil with Si^{8+}, energy ca. 100 MeV at 90^0 at the GPSC of the Pelletron at the IUAC, New Delhi, India, followed by chemical amplification of the damage trails by etching in 6 N NaOH, at 50 ± 2^0 C for 35 min. SEM photograph displaying the top view of the synthesized microstructures. Earlier it has been reported that if the dimensions of the pores were small, it would suppress the fractal like cauliflower morphology, which is a usual feature in electrodeposited II–VI materials (Klein et al 1993). In the present case, a close view of the microstructures depicting the typical cauliflower morphology of the synthesized CdS microstructures is obtained. In order to fabricate CdS nanowires in AAMs, the cathode of the two-electrode deposition cell was closely covered with gold coated AAMs. The cathode was made highly smooth and the electrolyte and deposition conditions were maintained same as described for deposition through TEMs.
[Sangeeta, Kumar, V. **GENERATION OF NANO-/MICROSTRUCTURES OF CdS AND ZnO USING ELECTRODEPOSITION AND THEIR CHARACTERIZATION.** J *Am Sci* 2022;18(5):1-9]. ISSN 1545-1003 (print); ISSN 2375-7264 (online). http://www.jofamericanscience.org. 1. doi:10.7537/marsjas180522.01.

Keywords: Templates, Nano/Microstructure, Electrodeposition, CdS and ZnO

Introduction:

In recent years, there has been a rapid development in the field of II – VI group semiconductor nano-/microstructures, especially chalcogenides and oxides. Semiconductor nanostructures exhibit novel physical properties which make them suitable for potential applications in nanoscale electronics, optoelectronic devices, high –density magnetic memories, electrochemical and sensing devices (Cobden 2001**;** Ma et al 2003 ; Fasol 1996; Stafford et al 1997; Hoppleer and Zwrger1999; Prinz 1998; Li et al 1997). The present study includes the fabrication of the II-VI group semiconductor compounds CdS and ZnO. CdS finds its applications as an important material for functional nanodevices such as light emitting diodes, sensors, solar cells (Kang and Kim 2006**),** thin film field effect transistors (Duan et al 2003), photoconductors, and optoelectronic devices (Woggon et al 1993). CdS is a well known n-type wide direct band gap II-VI semiconductor with E_g= 2.42 eV at room temperature. So far, a variety of techniques such as physical vapor deposition (Wu and Tao 2002), chemical solution transport growth (Zhan et al 2000, Zhang et al 2002), solvothermal synthesis, sulfurization (Fan et al 2002), microwave assisted growth (Yonghong et al 2004), thermal evaporation (Zhang et al 2006) and electrodeposition (Enculescu et al 2005, Kang and Kim 2006)) have been used to synthesize CdS nanowires. We report here the synthesis of CdS nano-/micro structures in TEMs and AAMs. The energy band gap (E_g) value of CdS nanowires were estimated by absorption spectra using Tauc relation. Laser induced pulse excitation method was used to study the photoluminescence spectra.

Another material of choice in present research was ZnO which is a well known n-type wide direct band gap semiconductor with E_g = 3.37 eV and large excitation energy (60 meV) at room temperature. ZnO is the most commonly studied material for functional nanodevices such as LEDs (Konenkamp et al 2004), gas sensors (Xu et al 2005, Wang et al 2006, Wan et al 2004), FETs (Fan et al 2004, 2006), piezoelectric-nanogenerators, gated diodes and resonators, field emitters (Liao et al 2005, Xu et al 2004, Zhao et al 2006), optical waveguides (Law et al 2004), dye-sensitized solar cells(Law et al

2005) and logic gates (Park et al 2005). Various growth mechanisms such as CVD (Bae et al 2004), direct thermal evaporation (Wang et al 2004), plasma-enhanced CVD (Liu et al 2004), metal – organic chemical vapor deposition MOCVD (Park et al 2002), electrochemical deposition (Leprince-Wang 2005), sol-gel deposition (Chen et al 2005), sonochemical and microwave-assisted (Hu et al 2004), surfactant assisted growth (Xu et al 2002) and hydrothermal processes(Liu and Zeng 2003) have been reported in literature to fabricate ZnO nanowires. We report here the fabrication of ZnO nanowires in AAMs using electrodeposition. The structural properties of the synthesized ZnO nanowires have been studied by SEM and XRD. Laser induced pulse excitation method was used to study the PL spectra.

Various types of electrodeposition cells have been used for synthesizing nano-/microstructures of metals (Penner and Martin 1987, Tierney and Martin 1989, Chakarvarti and Vetter 1991, Dobrev et al 1995). In general, a suitable cell offers a low ohmic voltage drop across the electrodes even if the cell is filled with poorly conducting electrolyte. The schematic diagram of the cell used in our laboratory is as shown in figure. The cell is a cylindrical structure made of perspex with a detachable cathode and anode assembly separated by a diaphragm of perspex sheet. For homogeneous growth of nano-/microstructures within the template, the anode is made preferably conical because for flat anodes, the material is deposited preferentially at the outer boarder areas of the cathode (Puippe and Leaman 1986). The area of anode is made much larger than the effective area of cathode in order to make anode overvoltage small compared to cathode overvoltage during deposition and anode is used at the same time as references electrode.

CdS microstructures in track etch templates

The membranes used here as templates were of Makrofol KG foil (polycarbonate from Bayer AG), 10 μm thick, having an average pore diameter ~2 μm with pore density 2×10^6 cm^{-2}. This was prepared by irradiating the foil with Si^{8+}, energy ca. 100 MeV at 90^0 at the GPSC of the Pelletron at the IUAC, New Delhi, India, followed by chemical amplification of the damage trails by etching in 6 N NaOH, at 50 ± 2^0 C for 35 min. In order to produce see-through pores, optimum etch time and etch conditions are pre-set. For the fabrication of the CdS microstructures in the form of columnar ensembles, the cathode (Al tape as substrate having its base coated with conducting adhesive) of the specially designed electrodeposition cell, having provisions for temperature control and stirring at different speeds, was covered closely with the processed TEM and the electrolyte solution to be used in the bath was prepared using milli Q 10-MΩ water and ultrahigh purity reagents 0.002M $3CdSO_4 \times 8H_2O$(98%) + 0.1M Na_2SO_3 (99.9%). The pH of the electrolyte was adjusted between 2-3 using dilute H_2SO_4. The galvanic replication was carried out for 50 min at 3.5 V at a room temperature of 29 ± 1^0C with an anode of pure Cd.

SEM Characterization

Images were recorded on the photographic film at different magnifications revealing the finer details of the microstructures and the etched pores of the host template. Fig 1 shows SEM photograph displaying the top view of the synthesized microstructures. Earlier it has been reported that if the dimensions of the pores were small, it would suppress the fractal like cauliflower morphology, which is a usual feature in electrodeposited II–VI materials (Klein et al 1993). In the present case, a close view of the microstructures depicting the typical cauliflower morphology of the synthesized CdS microstructures is obtained and shown in Fig 2. This is expected because of the fact that the pore size here was not in the nanorange. It has been reported (Bandyopadhyay and Miller 2000) that bright field high-resolution transmission electron microscopy of the materials deposited in the pores show a crystalline structure and crystallinity can further be increased by thermal annealing.

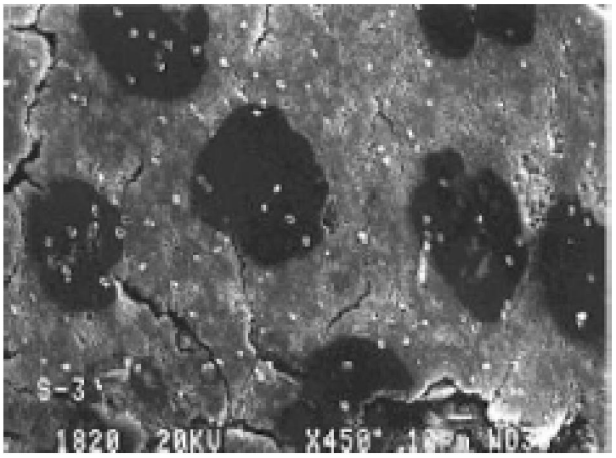

Fig. 1 Top view of the synthesized CdS microstructures

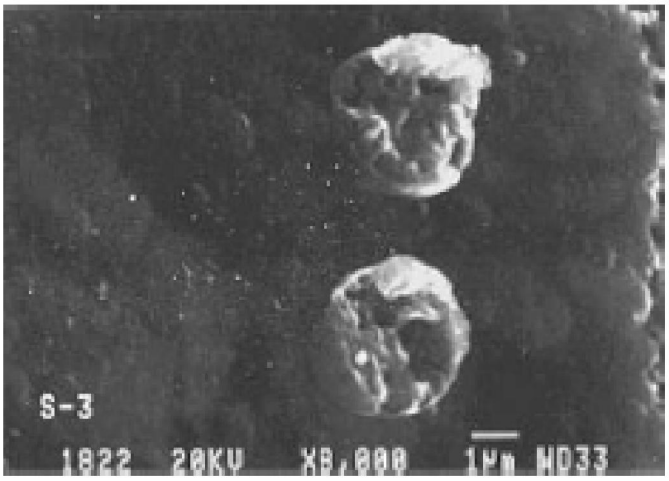

Fig. 2 Fractal-like cauliflower morphology of the synthesized CdS microstructures

CdS Nanowires in anodic alumina membranes

Commercially available AAMs having 20nm, 100nm pore diameters were used for electrodeposition of nanowires. In order to provide a conductive path for electrodeposition, a thin layer of gold ~100nm thick was deposited on the bottom surface of AAMs. In order to fabricate CdS nanowires in AAMs, the cathode of the two-electrode deposition cell was closely covered with gold coated AAMs. The cathode was made highly smooth and the electrolyte and deposition conditions were maintained same as described for deposition through TEMs. The membrane supported electrodeposition process is shown in Fig 3.

Fig. 4 shows the current vs time response for potentiostatic deposition of CdS nanowires of 100nm (a) and 200nm (b). The current vs time graph show that the deposition of nanowires is not a steady state process. After applying the potential, the current dropped suddenly due to creation of diffusion layer within the pores of template and afterwards the current gradually increases during the growth of nanowires in the template and attains a steady state when the filling reached the top of template. As soon

as caps start to cultivate on the top of structure, the current starts increasing slowly which increases rapidly with the increase of surface area of the caps due to overdeposition.

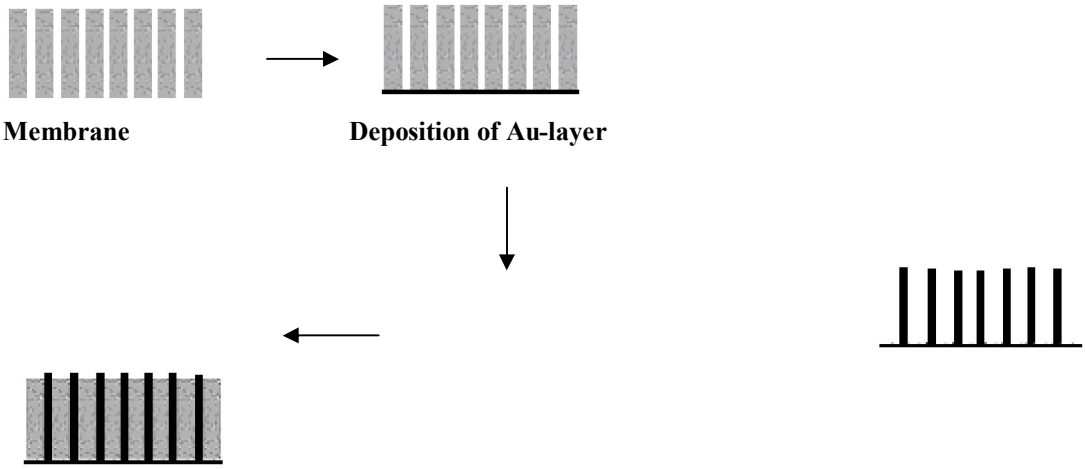

Fig. 3 Membrane supported electrodeposition process Arrays of nano-/micro structures and retrieved after dissolution of membrane.

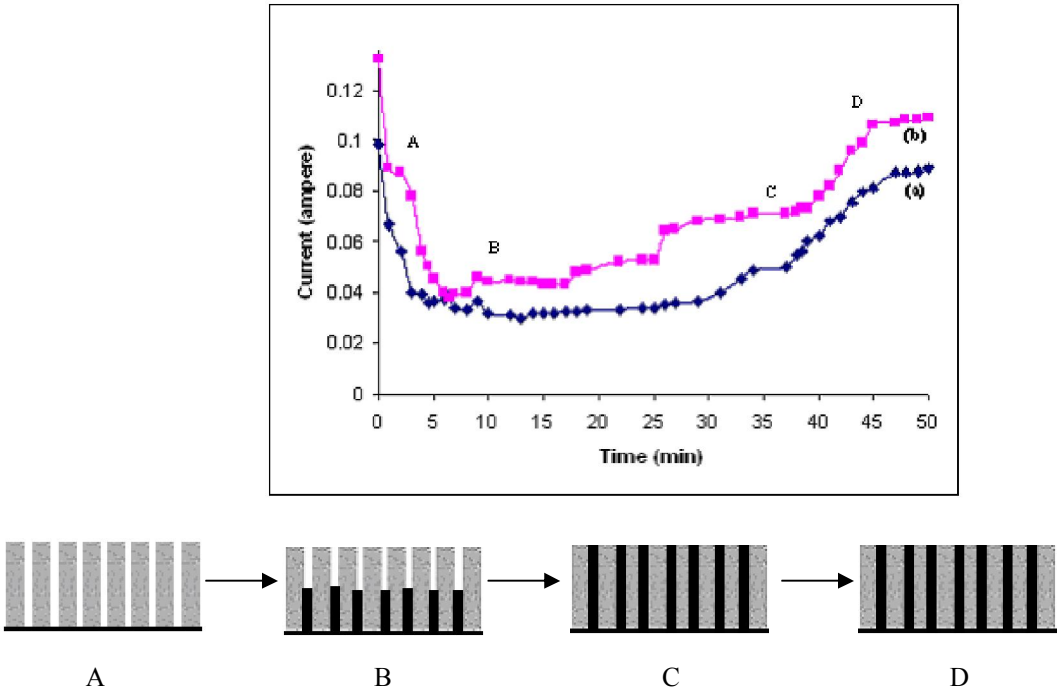

Fig. 4 Current vs time response for potentiostatic deposition of CdS nanowires of 100nm (a) and 200nm (b)

Structural csharacterization of CdS nanowires

After the deposition was over, the nanowires were released for further investigation, by dissolving the AAMs in 1M NaOH solution for 1 h followed by rinsing with double distilled water. Figures 5 and 6 show the photographs of CdS nanowires viewed

under scanning electron microscope operated at 10kV.

Optical characterization of CdS nanowires

The fundamental optical property of CdS nanowires investigated here is the absorption spectra at various wavelengths using UV-visible spectrophotometer. Fig 7 and 8 show the absorption spectra of CdS nanowires of 100 and 200nm respectively. The energy band gap of CdS nanowires is determined from absorption spectra using Tauc relation:

$$\alpha h\nu = A (h\nu - E_g)^n ,$$

Where α, $h\nu$, E_g, n and A have usual meanings as described earlier in Chapter-I.

The graphs between $(\alpha h\nu)^2$ vs $h\nu$ for CdS nanowires of 100 and 200nm are shown in figure 9 and 10 respectively. The presence of single slope in curve (fig. 9) indicates the direct and allowed transitions. The extrapolation of straight line to $h\nu$ axis gives value of energy gap value of CdS. The slight increase in band gap of nanowires is observed as the diameter of nanowires varies from 200nm to 100nm.

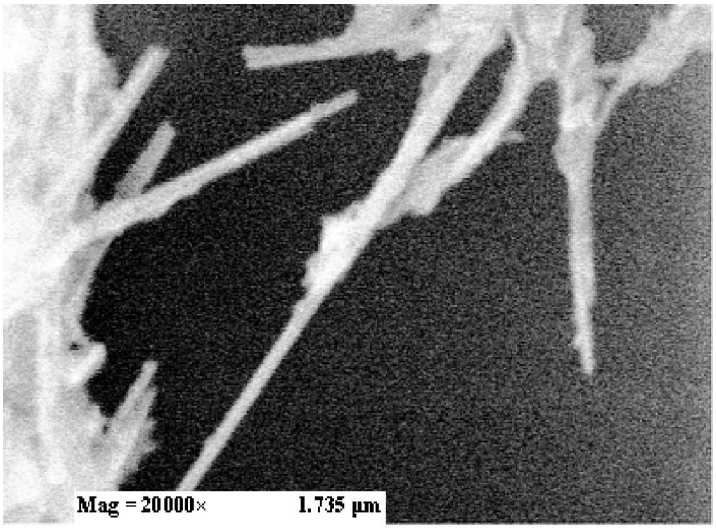

Fig. 5 SEM photographs of CdS nanowires (100nm)

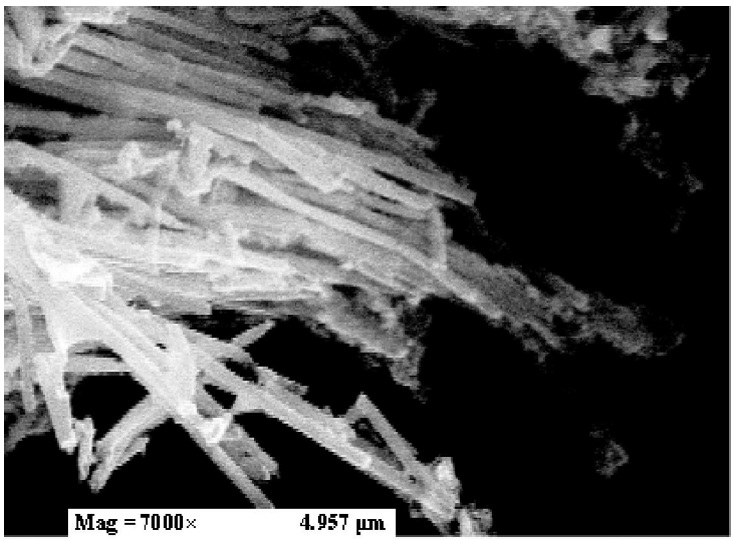

Fig.6 SEM photographs of CdS nanowires (200nm)

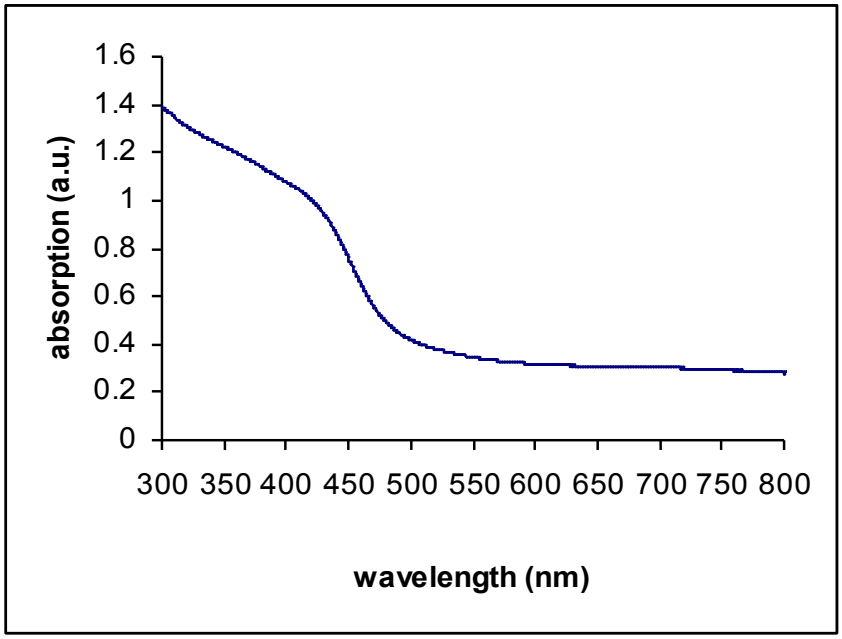

Fig. 7 Plot of absorption (α) versus wavelength (λ) for CdS nanowires (100nm)

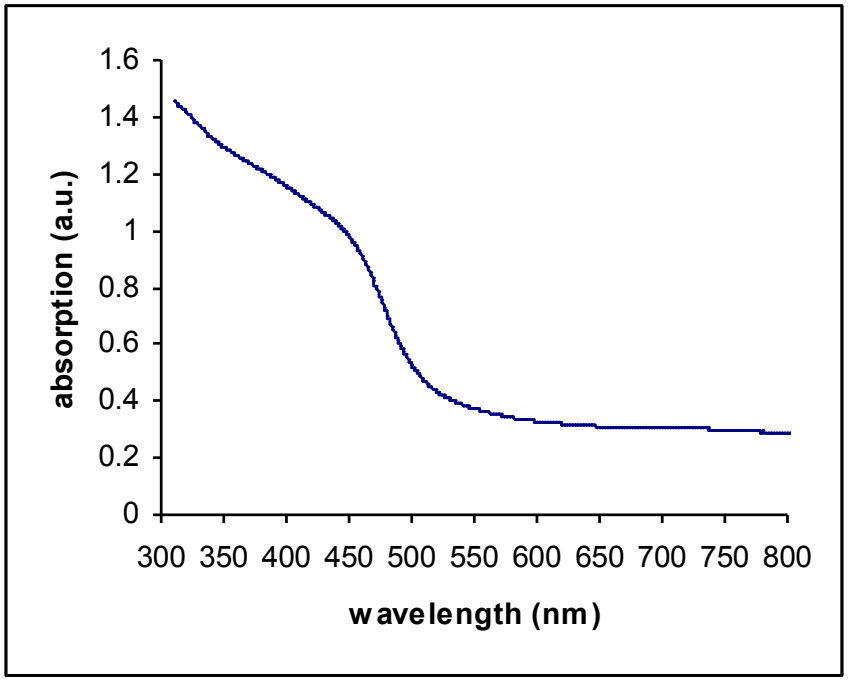

Fig. 8 Plot of absorption (α) versus wavelength (λ) for CdS nanowires (200nm)

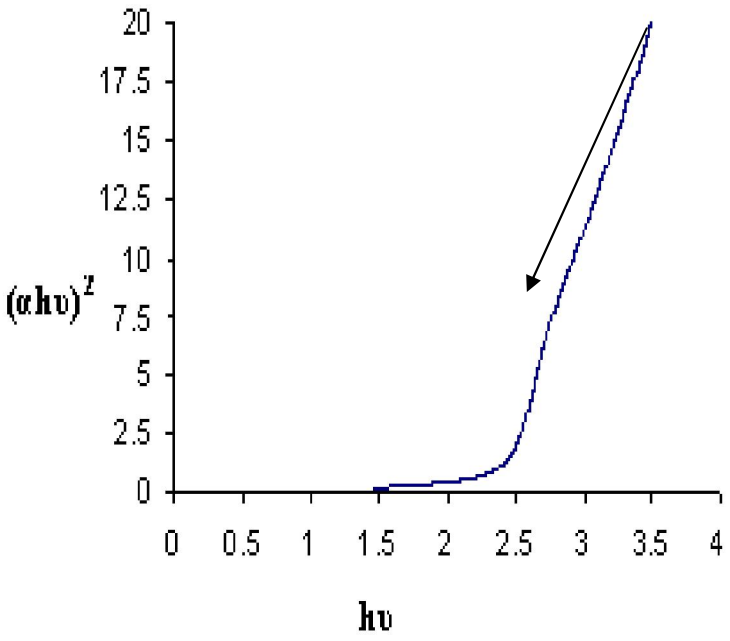

Fig. 9 Plot of $(\alpha h\upsilon)^2$ versus hυ (Tauc plot with dotted line is a theoretical fit) for CdS nanowires (200nm)

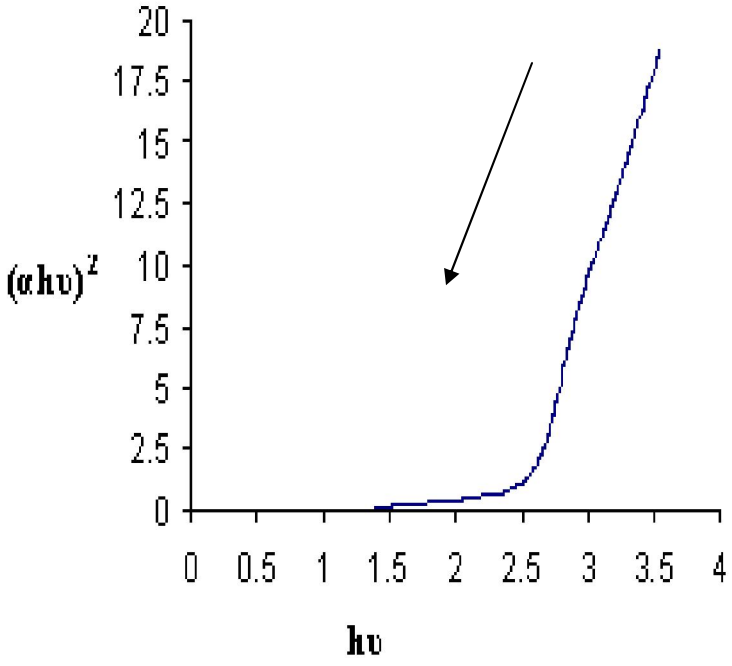

Fig. 10 Plot of $(\alpha h\upsilon)^2$ versus hυ (Tauc plot with dotted line is a theoretical fit) for CdS nanowires (100nm)

Photoluminescence (PL) study of CdS nanowires

Further, laser induced time resolved photoluminescence was used to study the photoluminescence spectra of 100 and 200nm CdS nanowires. The decay signals (Fig. 11 and 12) from the CdS nanowires were recorded for calculating emission wavelength of the nanowires. Photoluminescence investigation shows that the 200 nm CdS nanowires have an intensive and broad PL emission band peaked around 435 nm and with decrease in the size of CdS nanowires to 100 nm only slight variation is observed in the photoluminescence wavelength i.e 420 nm which shows that the electrons movement is slightly confined due to the size reduction but as the size of these wires is more than the Bohr exciton radius of CdS (5 nm), the quantum confinement is not observed. The results suggest that localized defects and excess S atoms existing in the CdS nanowires are responsible for this blue luminescence as no dopant had been added to the host of CdS nanowires.

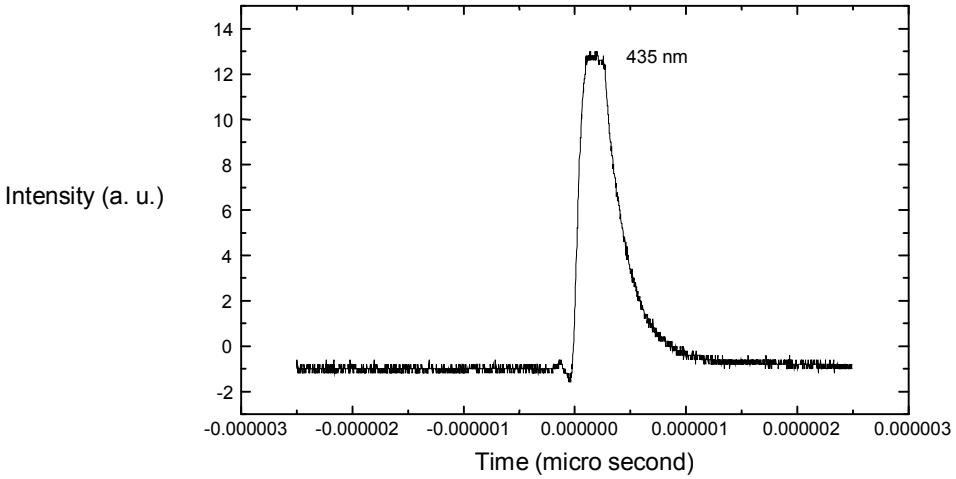

Fig. 11 Decay curve of 200 nm CdS nanowires

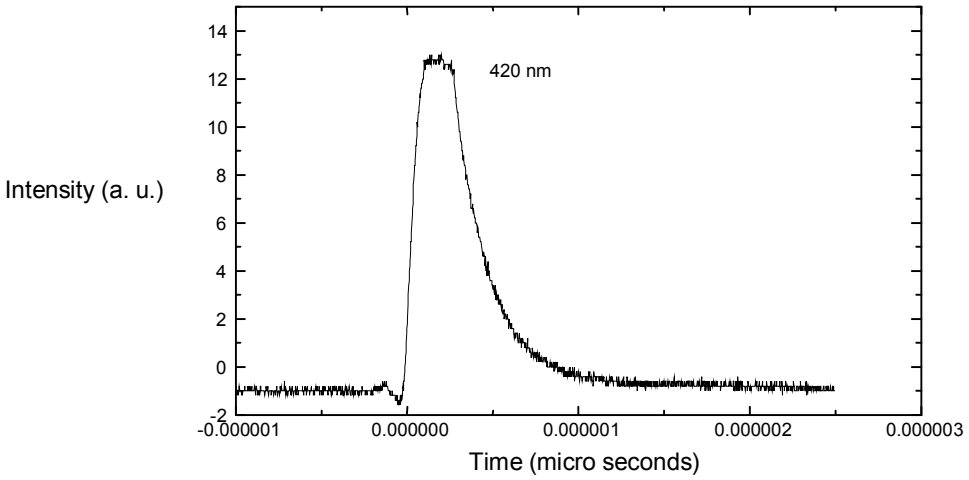

Fig. 12- Decay curve of 100 nm CdS nanowires

Bibliography

[1]. Abdelkader H. and H. John, and T. Luong (2000), "*Electrochemical detectors prepared by electroless deposition for microfabricated electrophoresis chips*", Anal. Chem., 72 (19), 4677 -4682.

[2]. Angert N. and C. Trautmann (1996), "*Swift heavy ion tracks in material*", Proceedings of the 7th International Symposium on Advanced Nuclear Energy Research Recent Progress in Accelerator Beam Application, Takasaki, Japan.

[3]. Ansermet J. P. (1998), "*Perpendicular transport of spin-polarized electrons through magnetic nanostructures*", J. Phys.: Condens. Matter, 10, 6027.

[4]. Cai, Z, J. Lei, W. Liang, V. Menon, and C. R. Martin (1991), "*Molecular and supermolecular origins of enhanced electronic conductivity in template-synthesized polyheterocyclic fibrils supermolecular effects*," Chem. Mater., 3, 960-967.

[5]. Calcote H. F. and D. G. Keil (1997), "*Combustion synthesis of silicon carbide powder*", In. Proc. of the Joint NSF-NIST Conf. on Nanoparticles.

[6]. Delvaux M. and S. D. Champagne (2003), "*Immobilization of glucose oxidase within metallic nanotube arrays for application to enzyme biosensors*", Biosensors and Bioelectronics, 18,943-951.

[7]. DeVito S. and C. R. Martin (1998), "*Toward colloidal dispersions of template-synthesized polypyrrole nanotubules*," Chem. Mater. 10, 1738-1741

[8]. Dez R., F. Tenegal, C. Reynaud, M. Mayne, X. Armand, and N. Herlin-Boime (2002), "*Laser synthesis of silicon carbonitride nanopowders; structure and thermal stability*", Journal of the European Ceramic Society, 22,16, 2969-2979.

[9]. Ding J., W. F. Miao, P. G. Mc Cormick, and R. Street (1995), "*Mechanochemical synthesis of ultrafine Fe powder*", Appl. Phys. Lett. 67, 3804-3806.

[10]. Green Todd A. (2007), "*Gold electrodeposition for microelectronics, optoelectronic and microsystem application*", Gold Bull. , 40, 2.

[11]. Greene L. E., M. Law, J. Goldberger, F. Kim, J. C. Johnson, Y. Zhang, R. J. Saykally, and P. D. Yang (2003), "*Low-temperature wafer-scale production of ZnO nanowire arrays*", Ang. Chemie 42, 26, 3031-3034.

[12]. Gromov A. A., U. Förter-Barth, and U. Teipel (2006), "*Aluminum nanopowders produced by electrical explosion of wires and passivated by non-inert coatings: Characterisation and reactivity with air and water*", Powder Technology, 164, 2, 111-115.

[13]. Jae-Hyung P., S. G. Oh, and B. W. Jo (2004), "*Fabrication of silver nanotubes using functionalized silica rod as templates*", Materials Chemistry and Physics, 87, 2-3, 301-310.

[14]. Jaya S., G. G. Khan and A. Basumallick (2007), "*Nanowires: properties, applications and synthesis via porous anodic aluminium oxide template*", Bull. Mater. Sci., 30, 3, 271–290.

[15]. Jiang W., M. Pal and F. Hans (2005), "*Rapid production of carbon nanotubes by high power laser abalation*", Journal of manufacturing science and engineering, 127, 3, 703-707.

[16]. Yonghong N., X. Ma, J. Hong, and Z. Xu (2004), "*Microwave-assisted template synthesis of an array of CdS nanotubes*", Materials Letters 58, 2754– 2756.

[17]. Yu S. H. (2001), "*Hydrothermal/solvothermal processing of advanced ceramic materials*", J. Ceram. Soc. JPN 109, 5, 65-75.

[18]. Zachariah M. R. (1994), "*Flame processing, in-situ characterization, and atomistic modeling of nanoparticles in the reacting flow group at NIST*", In Proc. Of the Joint NSF-NIST Conf. on Ultrafine Particle Engineering (May 25-27, Arlington, VA).

[19]. Zhan J. H. , X. G. Yang, S. D. Li, D. W. Wang, Y. Xie , and Y. T. Qian (2000), "*A chemical solution transport mechanism for one-dimensional growth of CdS nanowires*", Journal of crystal growth 220, 231-234.